Partial oxidation of methane to syngas over Ni/MgO, Ni/CaO and Ni/CeO_2

S. Tang, J. Lin * and K.L. Tan

Surface Science Laboratory, Department of Physics, National University of Singapore, 10 Kent Ridge Crescent, Singapore 119260
E-mail: phylinjy@leonis.nus.sg

Received 27 October 1997; accepted 25 February 1998

Partial oxidation of methane to syngas at atmospheric pressure and 750 °C was examined over Ni/MgO, Ni/CaO and Ni/CeO_2 catalysts with nickel loading of 13 wt%. All catalysts had similar high conversion of methane and high selectivity to syngas, which nearly approached the values predicted by thermodynamic equilibrium. However, only Ni/MgO showed high resistance to carbon deposition under thermodynamically severe conditions ($CH_4/O_2 = 2.5$, a higher CH_4 to O_2 ratio than the stoichiometric ratio). Its catalytic activity remained stable during 100 h of reaction, with no detectable carbon deposition. The oxidation of carbon deposited from pure CH_4 decomposition and from pure CO disproportionation was investigated by *in situ* TPO-MS study which showed that both were effectively inhibited over Ni/MgO. In addition, the catalysts were characterized by TPR, XRD and XPS. It was revealed that the excellent performance of Ni/MgO resulted from the formation of an ideal solid solution between NiO and MgO.

Keywords: partial oxidation of methane (POM), syngas, nickel catalyst, carbon deposition

1. Introduction

In the past decade, considerable attention has been paid to the direct conversion of methane, such as oxygenation to methanol and formaldehyde [1] and oxidative coupling of methane to ethylene and ethane [2,3]. Unfortunately, it is difficult to utilize these processes at industrial scale because of low yields of useful products. An alternative route is to convert methane into syngas (CO and H_2) which is then further converted to higher hydrocarbons and oxo compounds.

The dominant industrial process for the production of syngas is steam reforming of methane:

$$CH_4 + H_2O \rightarrow CO + 3H_2, \quad \Delta H = 225.4 \text{ kJ/mol} \quad (1)$$

This reaction is strongly endothermic and needs superheated steam in excess ($H_2O/CH_4 \approx 2$–3) in the feed gases in order to inhibit carbon deposition on nickel catalysts. Therefore, it is a highly energy-consuming and capital-intensive process. It provides higher H_2/CO ratio (>3) feedstocks than those for Fischer–Tropsch synthesis and the production of methanol. However, the partial oxidation of methane (POM) to syngas is mildly exothermic and energy efficient:

$$CH_4 + (1/2)O_2 \rightarrow CO + 2H_2, \quad \Delta H = -22.6 \text{ kJ/mol} \quad (2)$$

It also produces syngas of more desirable stoichiometric ratio ($H_2/CO \approx 2$) suitable for the methanol and Fischer–Tropsch syntheses. Moreover, the combustion system in the steam-reforming process gives off pollutant gases (NO_x, CO, SO_x, CO_2). These waste gases may be eliminated in the POM process, which would stimulate additional interest from the standpoint of environmental protection [4].

Recently, a number of papers on partial oxidation of methane to syngas with high conversion of methane and good selectivities to CO and H_2 have been published, with supported nickel [5–8], supported noble metals [9–14], or pyrochlore and perovskite oxides [15–20] being the catalysts. In the production of syngas from CH_4, coke formation over the catalyst frequently takes place, resulting in catalyst deactivation or the plugging of reactor. Carbon deposition mainly comes from methane decomposition ($CH_4 \rightarrow C_{(s)} + 2H_2$) and CO disproportionation reaction ($2CO \rightarrow C_{(s)} + CO_2$), where $C_{(s)}$ refers to solid carbon. Traditional supported nickel catalysts used in steam reforming of methane have shown substantial carbon deposition for POM [21]. Although supported noble metals (Ru, Rh, Pt, Ir) and the pyrochlore and perovskite oxides-containing noble metals have possessed excellent resistance to carbon deposition [15,16,21], their use in this process is limited because of their extremely high cost. Therefore, it is desirable to develop novel supported nickel catalysts with good resistance to coke. Takashi et al. reported that $Ni/Ca_{1-x}Sr_xTiO_3$ catalyst prepared by the citrate method from perovskite precursors showed high resistance to coke generation using air as oxidant [19]. Choudhary et al. [12–14] studied a series of mixed oxide catalysts NiO/MO_x (M = Ca, Mg, lanthanides with $Ni/M \geqslant 1$) used in oxidative conversion of methane and found that all NiO/MO_x catalysts had similar high activity and selectivity at low-temperature range (300–700 °C) and extremely high space velocities. Ruckenstein and Hu had also studied Ni/alkaline earth metal oxide catalysts, which were nevertheless used for the methane

* To whom correspondence should be addressed.

reforming with CO_2 to syngas. It was found that only Ni/MgO showed good activity and excellent stability [22–24]. To test whether Ruckenstein and Hu's conclusion is also applicable to the partial oxidation of methane, we prepared Ni/MgO, Ni/CaO and Ni/CeO_2 catalysts with nickel loading of 13 wt%, and investigated their activity and carbon deposition, as well as their stability for POM. The structures of catalysts were also probed using TGA, TPR, XRD and XPS.

2. Experimental

2.1. Preparation of the catalysts

The catalysts were prepared by impregnating metal oxides with an aqueous solution of nickel nitrate. Before impregnation, as-received MgO and CeO_2 were calcined at 600 °C for 3 h, while CaO was obtained by decomposing calcium carbonate at 950 °C for 2 h. The impregnated materials in a thick paste were dried in an oven at 100 °C for 24 h and then decomposed in air at 600 °C for 15 h. The decomposed mass was pressed binder-free to pellets and calcined in air at 900 °C for 3 h. The content of nickel was 13 wt% for all catalysts.

2.2. Catalytic reaction

The catalytic reaction was carried out under atmospheric pressure, at 750 °C, in a continuous flow quartz microreactor (I.D. 4 mm) packed with 100 mg catalysts (20–35 mesh size). The catalysts were reduced in a flow of H_2 (20 ml/min) at 700 °C for 1 h, and feed gases with fixed CH_4/O_2 ratio and gas hourly space velocity (GHSV) were passed through the catalyst bed immediately after the hydrogen was turned off at 750 °C. The reaction products were analyzed with an *in situ* gas chromatograph equipped with a Porapak Q column. To separate O_2 and CO, a mass spectrometer was also used to monitor the oxygen in the products, which showed that the oxygen was completely converted under selected reaction conditions.

Since carbon deposition on catalysts occurred easily at high ratio of CH_4 to O_2 [8], feedstocks with CH_4 to O_2 in the ratio of 2.5 : 1 were used. For comparison, the measurement of catalytic activity of all catalysts, as well as the stability test of Ni/MgO, was also conducted with a stoichiometric ratio of $CH_4/O_2 = 2$. A suitable space velocity was taken (GHSV $\approx 5.6 \times 10^4$ $cm^3\,g^{-1}\,h^{-1}$) so that harsh hot spots were avoided. According to the experimental results reported by Tsang et al. [25], the difference of temperature in the catalyst bed of Ni/MgO catalyst is about 30 °C at the space velocity we used. We have also measured the temperature distribution in the catalyst bed by placing a thermocouple directly at various parts of the catalyst bed. The temperature in the top layer of the catalyst bed was found to be about 35 °C higher than that at the other places in the catalyst bed. Therefore, the harsh hot spots were eliminated in this experiment.

2.3. Characterization of catalysts

The amount of carbon deposited on catalysts during POM reaction was measured *ex situ* by thermogravimetric analysis (Perkin-Elmer TGA 7) and mass spectrometry (Balzers QME 200). The weight change of catalysts was monitored by TGA while the resulting CO_2 and CO were detected by an on-line mass spectrometer when the carbon was burned out by diluted oxygen (10% O_2/Ar) in a temperature-programmed process from 25 to 900 °C (30 °C/min). However, for studying the carbon deposition from pure CH_4 decomposition and from pure CO disproportionation the experiment was performed *in situ* in the following manner: either pure CH_4 or pure CO (20 ml/min) was passed through the catalysts (50 mg) for 20 min at 750 °C after the catalysts were reduced in a flow of H_2 for 30 min at 700 °C and purged by He for 20 min at 750 °C. The catalyst sample was then cooled down to 80 °C in a flow of He and temperature-programmed oxidation (TPO) was carried out in a 10% O_2/Ar gas stream with temperature linearly increased from 80 to 800 °C at a rate of 15 °C/min. The CO_2 and CO produced were detected by an on-line mass spectrometer which was calibrated by monitoring the decomposition of weighted amounts of calcium carbonate.

Temperature-programmed reduction (TPR) of the catalysts was performed by heating the samples from room temperature to 800 °C at rate of 15 °C/min, in a 10% H_2/Ar gas flow (45 ml/min). The sample (100 mg in all runs) was pretreated in a flow of He so that the absorbed gases were removed before the TPR. The response was measured using a thermal conductivity detector connected to a recorder.

X-ray powder diffraction (XRD) was carried out on a Philips PW 1710 X-ray diffraction spectrometer using a Cu Kα radiation source.

X-ray photoelectron spectroscopy (XPS) analysis was undertaken on a VG ESCALAB MK II spectrometer, using a Mg Kα X-ray source (1253.6 eV, 120 W). Analyzer pass energy of 20 eV was adopted for all narrow scans. The binding energies were calibrated with the C(1s) level of adventitious carbon (284.5 eV) as the internal standard reference. The ratios of atoms on the surface of catalysts were calculated using the following formula:

$$n_1/n_2 = \frac{I_1/S_1}{I_2/S_2},$$

where I_i is the XPS peak area and S_i the atomic sensitivity factor of the corresponding element.

3. Results

3.1. Catalytic activity and carbon deposition

The catalytic activities of the Ni/MgO, Ni/CaO and Ni/CeO_2 catalysts with stoichiometric feed gases ($CH_4/O_2 = 2$), GHSV $= 5.6 \times 10^4$ $cm^3\,g^{-1}\,h^{-1}$ and reaction temperature of 750 °C are displayed in table 1. It is seen that

Table 1
Catalytic activity of catalysts for the partial oxidation of methane to syngas ($CH_4/O_2 = 2$, GHSV $= 5.6 \times 10^4$ cm^3 g^{-1} h^{-1}, $T = 750\,^\circ$C).

Catalyst	CH_4 conversion (%)	CO selectivity (%)	H_2 selectivity (%)
Ni/MgO	91.2	92.4	96.3
Ni/CaO	90.9	92.3	96.5
Ni/CeO_2	91.6	93.3	96.0
Thermodynamic equilibrium [25]	91.7	96.8	97.4

Table 2
Catalytic activity and carbon deposition on catalysts at higher ratio of CH_4 to O_2 ($CH_4/O_2 = 2.5$, GHSV $= 5.4 \times 10^4$ cm^3 g^{-1} h^{-1}, $T = 750\,^\circ$C).

Catalyst	CH_4 conversion (%)	CO selectivity (%)	H_2 selectivity (%)	Average rate of coke deposition[a] $\times 10^2$ (g(carbon) g^{-1} h^{-1})
Ni/MgO	81.9	95.4	98.0	0.06[b]
Ni/CaO	82.8	95.3	98.5	2.32[c]
Ni/CeO_2	83.3	96.1	97.1	2.22[c]

[a] Total reaction time = 6 h. [b] Obtained from MS analysis. [c] Obtained from TGA.

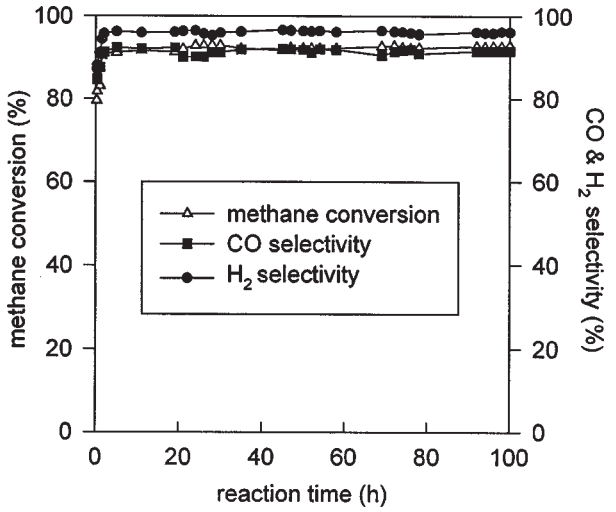

Figure 1. Catalytic activity and stability over Ni/MgO: $CH_4/O_2 = 2$, GHSV $= 5.6 \times 10^4$ cm^3 g^{-1} h^{-1}, $T = 750\,^\circ$C.

Ni/MgO, Ni/CaO and Ni/CeO_2 all show high activity and selectivity in the partial oxidation of methane to syngas. Both methane conversion and selectivity to syngas nearly approach the thermodynamic equilibrium values while oxygen is found to be completely consumed.

In order to efficiently investigate the carbon deposition on catalysts, feedstocks with a high ratio of $CH_4/O_2 = 2.5$ were used. As shown in table 2, although the catalysts have little difference from each other in their activity and selectivity, the amount of carbon deposition on Ni/MgO is much less than those on Ni/CaO and Ni/CeO_2. Note that carbon deposition was measured by TGA for Ni/CaO and Ni/CeO_2, whereas for Ni/MgO it was too little to be accurately determined by TGA and was therefore measured by MS. Owing to carbon deposition, the Ni/CaO and Ni/CeO_2 catalysts become partially shattered whereas Ni/MgO still shows good mechanical strength after reaction for 6 h. These have shown excellent resistance of Ni/MgO to carbon deposition even under thermodynamically severe conditions (high ratio of CH_4 to O_2).

Table 3
The amount of carbon deposition from pure CH_4 decomposition and pure CO disproportionation (catalyst amount = 50 mg, $T = 750\,^\circ$C, flow rate = 20 ml/min, reaction time = 20 min).

Catalyst	Carbon deposition (wt%)	
	CH_4 decomposition	CO disproportionation
Ni/MgO	2.37	0.60
Ni/CaO	6.04	5.31
Ni/CeO_2	9.80	4.28

To further investigate the stability of Ni/MgO for POM, a test was conducted with stoichiometric feed gases ($CH_4/O_2 = 2$) and GHSV $= 5.6 \times 10^4$ cm^3 g^{-1} h^{-1} at 750 °C. The results show that its catalytic activity remains stable during 100 h on stream (see figure 1) and no coke deposition has been observed even after reaction for 100 h.

In order to probe the origin of the deposited carbon, carbon deposition from pure methane decomposition and from CO disproportionation was investigated. The results are summarized in table 3. The amount of the carbon deposited from pure CH_4 decreases in the order of Ni/CeO_2 > Ni/CaO > Ni/MgO while that from pure CO follows the trend of Ni/CaO > Ni/CeO_2 > Ni/MgO. It is noted that the carbon deposition from CO is more effectively suppressed over Ni/MgO. Figures 2 and 3 are the TPO profiles of the deposited carbon over Ni/MgO (a), Ni/CeO_2 (b) and Ni/CaO (c) from pure CH_4 and pure CO, respectively. As described in the experimental section, they were obtained by using *in situ* mass spectrometry to measure the intensity of CO_2, the product of the oxidation of the deposited carbon, as a function of linearly increased sample temperature. In addition to the smaller quantity, figures 2 and 3 also reveal that the oxidative temperature of carbon deposited on Ni/MgO is lower than those of carbon deposited on Ni/CeO_2 and Ni/CaO.

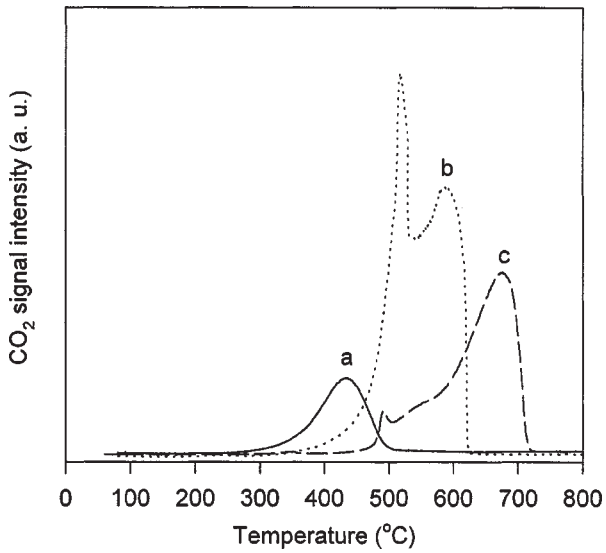

Figure 2. TPO profiles of the carbon deposited from CH_4 decomposition over: (a) Ni/MgO; (b) Ni/CeO_2; (c) Ni/CaO.

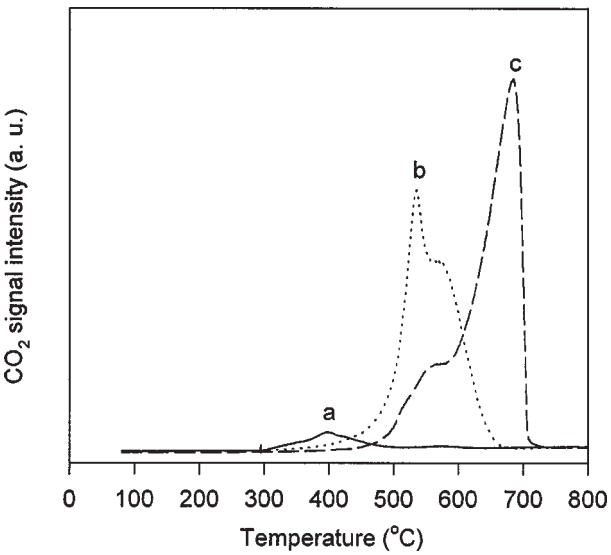

Figure 3. TPO profiles of the carbon deposited from CO disproportionation over: (a) Ni/MgO; (b) Ni/CeO_2; (c) Ni/CaO.

3.2. Temperature-programmed reduction (TPR)

The H_2-TPR results of the catalysts are given in figure 4, which shows a broad and strong peak of reduction at about 360 °C for Ni/CaO (a), and a strong peak at 360 °C and a weak peak at 510 °C for Ni/CeO_2 (b). In contrast, only a very weak peak at 500 °C appears in the TPR of Ni/MgO (c). Combined with the XRD results shown below, this indicates that it is difficult to reduce the NiO in Ni/MgO catalyst and only a small amount of NiO can be reduced to metallic nickel.

3.3. Powder X-ray diffraction (XRD)

XRD analysis has been carried out for Ni/MgO, Ni/CaO and Ni/CeO_2, in both freshly prepared and H_2-reduced

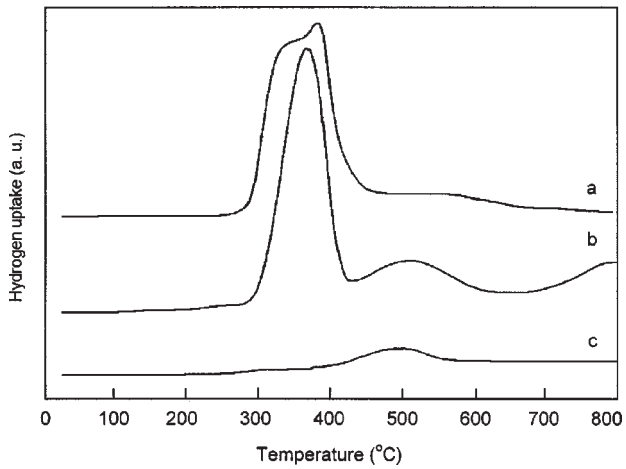

Figure 4. The H_2-TPR profiles of catalysts for: (a) Ni/CaO; (b) Ni/CeO_2; (c) Ni/MgO.

states. The results show that there exist obvious NiO phases in fresh nickel catalysts supported on CaO and CeO_2. The fresh Ni/CaO catalyst consists of NiO, CaO and a little $Ca(OH)_2$, and the fresh Ni/CeO_2 catalyst is composed of NiO and CeO_2. After Ni/CaO and Ni/CeO_2 catalysts were reduced in a flow of H_2 at 700 °C for 1 h, the peaks of NiO disappeared and were replaced by those of metallic nickel (see figure 5), indicating the complete reduction of NiO to Ni.

As for Ni/MgO, no distinguishable peaks of NiO are observed in fresh Ni/MgO catalyst (figure 6(b)). It should be noted that although NiO and MgO have similar XRD patterns, doublet peaks corresponding to NiO and MgO are present for the mechanical mixture of NiO and MgO without calcination (figure 6(a)). The fresh Ni/MgO catalyst prepared by impregnation has the same XRD pattern as that of pure MgO (figure 6 (b) and (c)), without doublet structure, indicating that NiO and MgO have formed a solid solution. When the Ni/MgO catalyst is subjected to the H_2 reduction at 700 °C for 1 h, the phase of metallic nickel is not detected (figure 6(d)). It is slightly detectable after the catalyst has been reduced and used in the POM reaction for 3 h (figure 6(e)). This reveals that the metallic nickel may be supported on MgO in an amorphous or a highly dispersed state. Therefore, the XRD analysis has shown a very different structure of Ni/MgO from those of Ni/CaO and Ni/CeO_2.

3.4. XPS analysis

Table 4 presents the molar ratios of nickel to metal atom (Mg, Ca or Ce) of support for the reduced catalysts. The surface Ni/Mg ratio of reduced Ni/MgO catalyst is almost the same as the bulk Ni/Mg molar ratio. The Ni/Ca and Ni/Ce molar ratio, however, are largely beyond their bulk molar ratio. Therefore, the surfaces of Ni/CaO and Ni/CeO_2 catalysts are enriched in nickel whereas nickel in Ni/MgO catalyst is more uniformly dispersed in the MgO support. It is generally suggested that the active component in sup-

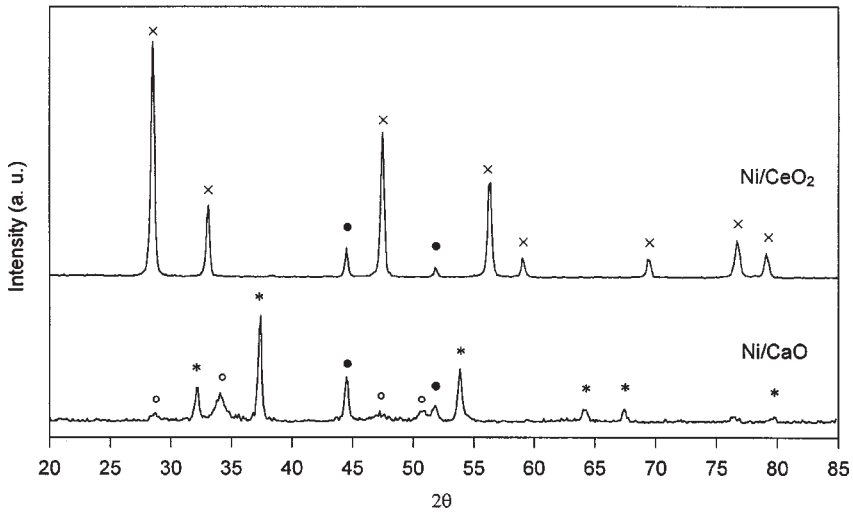

Figure 5. XRD patterns of Ni/CaO and Ni/CeO_2 after reduction in H_2 at 700 °C for 1 h: crystalline phase, (•) Ni; (∗) CaO; (○) $Ca(OH)_2$; (×) CeO_2.

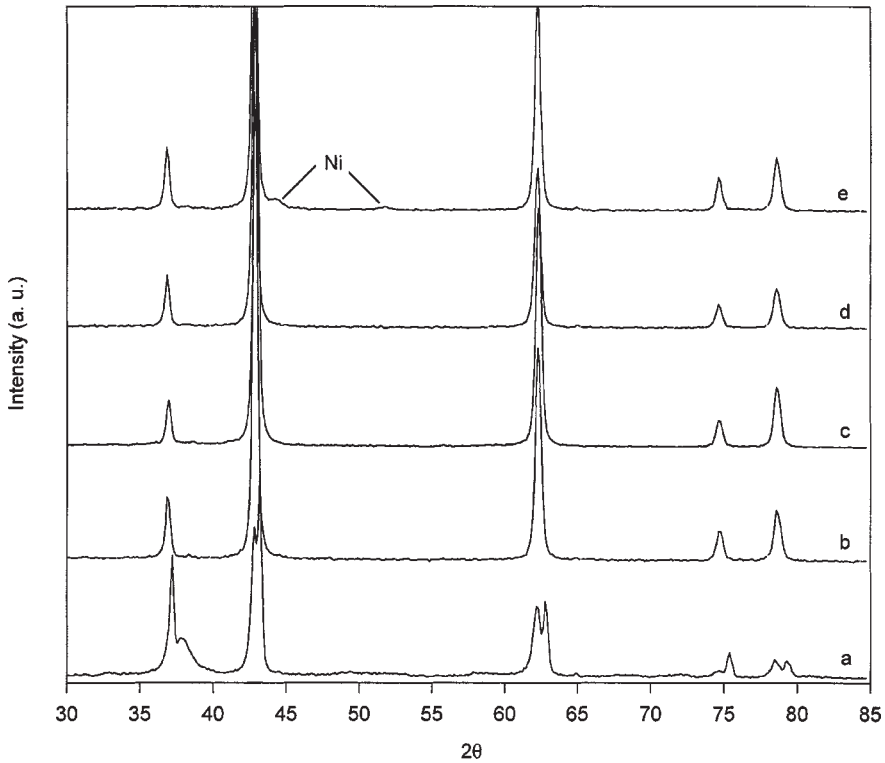

Figure 6. XRD patterns of NiO/MgO: (a) mechanical mixture of NiO and MgO without calcination; (b) fresh Ni/MgO catalyst prepared by impregnation; (c) pure MgO calcined in air at 900 °C for 3 h; (d) Ni/MgO catalyst reduced in H_2 at 700 °C for 1 h; (e) Ni/MgO catalyst after reduction and reaction for 3 h.

Table 4
The molar ratios of Ni/metal atom (Mg, Ca or Ce) of support derived from XPS data.

Catalyst	Ni/metal atom of support (molar ratio)		$R_{surface}/R_{bulk}$
	R_{bulk}[a]	$R_{surface}$	
Ni/MgO	0.102	0.105	1.03
Ni/CaO	0.142	0.522	3.67
Ni/CeO_2	0.430	1.580	3.68

[a] Calculated from weight ratios.

ported nickel catalysts for POM is metallic nickel [8]. The XPS spectra of Ni($2p_{3/2}$) for the reduced catalysts are displayed in figure 7, with the Ni^0 peak at 852.6 eV, Ni^{2+} at 854.5 eV and the shake-up intensity in the energy region between 858 and 866 eV. A strong Ni^0 signal was detected in the reduced Ni/CaO and Ni/CeO_2 catalysts even though they were exposed to air for several hours after reduction. However, a weak Ni^0 signal was found in the reduced Ni/MgO catalyst only when the sample was rapidly transferred to the XPS chamber after reduction. No Ni^0 was

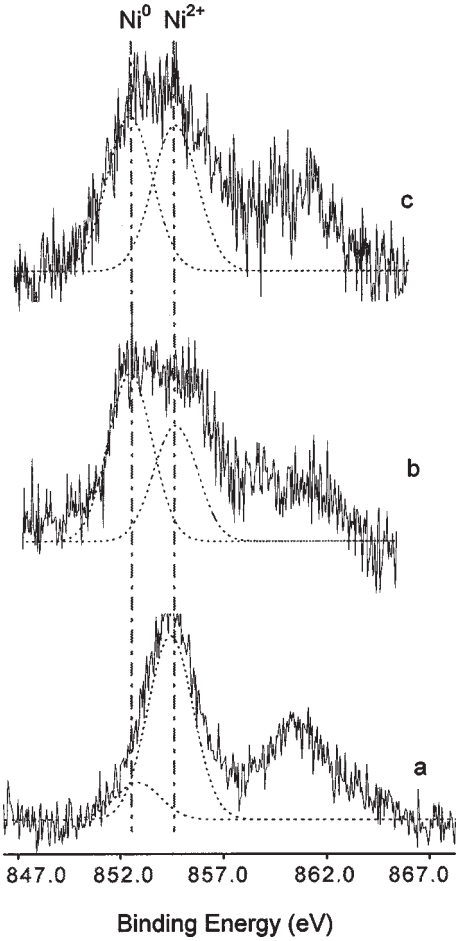

Figure 7. XPS spectra of Ni($2p_{3/2}$) for reduced catalysts: (a) Ni/MgO; (b) Ni/CaO; (c) Ni/CeO_2.

detected if it was exposed to air for minutes. The above XPS results further confirm that compared with Ni/CaO and Ni/CeO_2, only a small amount of NiO in Ni/MgO catalyst is reduced to metallic nickel.

4. Discussion

Although Ni/MgO, Ni/CaO and Ni/CeO_2 catalysts with nickel loading of 13 wt% show similar high catalytic activity and good selectivity for partial oxidation of methane, their resistance to carbon deposition is largely different from one another. Only Ni/MgO catalyst shows excellent resistance to carbon deposition under thermodynamically severe conditions and thus has a rather high stability. Experimentally, the carbon deposition from methane decomposition is observed to be suppressed over Ni/MgO (figure 2), which may be attributed to the strong ability for Ni/MgO to stabilize the CH_x intermediates with higher values of x [26–28]. Matsumoto observed different CH_x species during the adsorption of hydrocarbon on different nickel catalysts, i.e., $CH_{0.08}$ on nickel foil, $CH_{0.5}$ on Ni/SiO_2 and CH_2 on Ni/MgO, and he verified that CH_x species with lower values of x were more susceptible to form carbonaceous deposits [26,27]. Recently, using pulse surface reaction rate analysis Osaki et al. obtained $CH_{2.7}$ intermediate over Ni/MgO, $CH_{2.4}$ over Ni/Al_2O_3, $CH_{1.9}$ over Ni/TiO_2, $CH_{1.0}$ over Ni/SiO_2 for CH_4 reforming with CO_2 to syngas [28]. Hence, owing to the strong ability to stabilize high-x CH_x intermediates, the further decomposition of CH_x to produce carbon deposits is restrained. Another major carbon deposition process, the carbon deposition from CO disproportionation, is also more effectively inhibited over Ni/MgO (figure 3). In agreement with our results, Ruckenstein and Hu found, in their study of CO-TPD over nickel/alkaline earth metal oxides catalysts, that the reduced NiO/MgO produced a much smaller amount of CO_2 from CO than the reduced NiO/CaO and NiO/SrO did, namely, much less carbon deposition on reduced NiO/MgO [22].

As suggested by Ruckenstein and Hu, who studied the performance of Ni/MgO in methane reforming with CO_2 to syngas [22–24], the excellent resistance of Ni/MgO to carbon deposition most likely results from the formation of a solid solution between NiO and MgO. Because of similar crystalline structure (NaCl type) and approximate cation radii (Ni^{2+} 0.69 Å, Mg^{2+} 0.65 Å), NiO and MgO are completely miscible. They can form a solid solution through a mechanism of lattice substitution that leads to a system almost homogeneously "mixed" at high temperatures ($\geqslant$800 °C) [29,30]. The XRD patterns in figure 6(b) confirm that an ideal solid solution is formed in Ni/MgO catalyst. Compared with Ni/CaO and Ni/CeO_2, the formation of solid solution in Ni/MgO catalyst has a few unique advantages. Firstly, nickel can be more uniformly dispersed in the support, thus the segregation of nickel on the surface is avoided as revealed by XPS analysis (table 4). Secondly, as determined through TPR (figure 4), XRD (figure 6(d)) and XPS (figure 7), only a small portion of NiO can be reduced to Ni^0, which is strongly attached on the surface of MgO or partially inlaid in the lattice of MgO. Due to the small amount of Ni^0 and the strong interaction between Ni^0 and MgO, the aggregation of small Ni^0 particles is suppressed. In contrast, because NiO does not form solid solutions with CaO or CeO_2, almost all the NiO in Ni/CaO and Ni/CeO_2 is reduced to Ni^0 (figure 5) and the aggregation of Ni^0 easily occurs, generating relatively large Ni clusters responsible for coke formation [31]. Thirdly, since there exist strong interactions between the small nickel particles and MgO, the donor ability of nickel may be weakened [22]. It is well known that CO molecule is bound to a transition metal atom such as Ni through the donation of the lone pair electron density of the carbon atom to the vacant d orbital of the metal atom and the back donation of electron density from the filled d orbital of the metal to the vacant antibonding π* orbital of the CO molecule [32], the latter will weaken the CO bond and thus promote CO decomposition. From the above bonding scheme, the weaker donor ability of nickel in Ni/MgO largely hinders the CO disproportionation. In addition, the formation of a partially reducible NiO/MgO solid solution also directly increases the stability of Ni–Ni bonds on the reduced surfaces [33].

This greater surface stability prohibits nickel surface reconstruction via bond relaxation, hence carbon diffusion into the nickel lattice which leads to the formation of carbon whiskers may be prevented. From TPO profiles of deposited carbon, it is obvious that the carbon deposited on Ni/MgO is more easily oxidized. This indicates the aging of deposited carbon over Ni/MgO may be slowed down to some extent.

It is noticeable that Ni/MgO catalyst has high catalytic activity and stability even though only a small amount of NiO is reduced. As reported by Choudhary et al., NiO could be reduced in the POM reaction atmosphere at high temperatures ($\geqslant$600 °C) [5]. We also found that high activity of unreduced catalysts was gradually achieved in the exposure to the feed gases at 750 °C. Consequently, even if a little sintering of Ni^0 may occur, some Ni^0 produced through the reduction of NiO in the chemical atmosphere would make it up. At last, an equilibrium between Ni^0 and NiO is established, and thus its stability is maintained.

5. Conclusion

Ni/MgO, Ni/CaO and Ni/CeO_2 all have high catalytic activity and good selectivity for partial oxidation of methane to syngas. However, only Ni/MgO shows excellent resistance to carbon deposition and thus has a rather high stability. Due to the formation of a solid solution between NiO and MgO in Ni/MgO catalyst, it shows low reducibility, uniform dispersion and weak donor ability of nickel. As a result, carbon deposition, especially from CO disproportionation, is effectively inhibited over Ni/MgO catalyst.

References

[1] R. Pitchai and K. Klier, Catal. Rev. 28 (1986) 13.
[2] J.X. Wang and J.H. Lunsford, J. Phys. Chem. 90 (1986) 5883.
[3] G.J. Hutchings, M.S. Scurell and J.R. Woodhouse, Chem. Soc. Rev. 18 (1989) 25.
[4] N. Nichio, M. Casella, O. Ferretti, M. Gonzálaz, C. Nicot, B. Moraweck and R. Frety, Catal. Lett. 42 (1996) 65.
[5] V.R. Choudhary, A.S. Mamman and S.D. Sansare, Angew. Chem. Int. Ed. Engl. 31 (1992) 1189.
[6] V.R. Choudhary, A.M. Rajput and B. Prabhakar, Catal. Lett. 15 (1992) 363.
[7] V.R. Choudhary, V.H. Rane and A.M. Rajput, Catal. Lett. 22 (1993) 289.
[8] D. Dissanayake, M.P. Rosynek, K.C.C. Kharas and J.H. Lunsford, J. Catal. 132 (1992) 117.
[9] P.D.F. Vernon, M.L.H. Green, A.K. Cheetham and A.T. Aschroft, Catal. Lett. 6 (1990) 181.
[10] A.K. Bhattacharaya, J.A. Breach, S. Chand, D.K. Ghorai, A. Hartridge, J. Keary and K.K. Mallick, Appl. Catal. A 80 (1992) L1.
[11] J.A. Lapszewicz and X.Z. Jiang, Prepr. Am. Chem. Soc. Div. Petrol. Chem. 37 (1992) 252.
[12] L.D. Schmidt and D.A. Hichman, Science 259 (1993) 343; J. Catal. 138 (1992) 267.
[13] D.A. Hickman, E.A. Haufear and L.D. Schmidt, Catal. Lett. 17 (1993) 223.
[14] P.M. Tornianan, X. Chu and L.D. Schmidt, J. Catal. 146 (1994) 1.
[15] A.T. Ashcroft, A.K. Cheetham, J.S. Food, M.L.H. Green, C.P. Gray, A.G. Murrell and P.D.F. Vernon, Nature 344 (1990) 319.
[16] R.H. Jones, A.T. Aschroft, D. Waller, A.K. Cheetham and J.M. Thomas, Catal. Lett. 8 (1991) 169.
[17] Å. Slagtern and V. Oslbye, Appl. Catal. A 110 (1994) 99.
[18] T. Hayakawa, A.G. Andersen, M. Shimizu, K. Suzuki and K. Takehira, Catal. Lett. 22 (1993) 307.
[19] T. Hayakawa, H. Harihara, A.G. Anderson, A.P.E. York, K. Suzuki, H. Yasuda and K. Takehira, Angew. Chem. Int. Ed. Engl. 35 (1996) 192.
[20] V.R. Choudhary, B.S. Uphade and A.A. Belhekar, J. Catal. 163 (1996) 312.
[21] J.B. Claridge, M.L.H. Green, S.C. Tsang, A.P.E. York, A.T. Ashcroft and P.D. Battle, Catal. Lett. 22 (1993) 299.
[22] E. Ruckenstein and Y.H. Hu, Appl. Catal. A 133 (1995) 149.
[23] Y.H. Hu and E. Ruckenstein, Catal. Lett. 36 (1996) 145.
[24] Y.H. Hu and E. Ruckenstein, Catal. Lett. 43 (1997) 43.
[25] S.C. Tsang, J.B. Claridge and M.L.H. Green, Catal. Today 23 (1995) 3.
[26] H. Matsumoto, Shokubai 16 (1974) 122; 18 (1976) 71.
[27] H. Matsumoto, Hyomen 15 (1977) 226.
[28] T. Osaki, H. Masuda and T. Mori, Catal. Lett. 29 (1994) 33.
[29] H.B. Nussler and O. Kubaschewski, Z. Phys. Chem. N. F. 121 (1980) 187.
[30] F. Arena, B.A. Horrell, D.L. Cocke, A. Parmaliana and N. Giordano, J. Catal. 132 (1991) 58.
[31] J.R. Rostrup-Nielsen, J. Catal. 85 (1984) 31.
[32] R.R. Ford, Adv. Catal. 21 (1970) 51.
[33] M.C.J. Bradford and M.A. Vannice, Appl. Catal. A 142 (1996) 73.